frequency ultrasound can lyse very small clots without the help of lytic agents. They develop a method to declot full-size arteriovenous dialysis grafts in animals. Three declotting techniques were randomly applied: 1) direct injection of PESDA; 2) direct injection of saline; and 3) intravenous PESDA. Declotting was graded by cine-angiography score. Results showed high mean patency scores for direct PESDA and for IV PESDA vs. saline. Ultrasound in this case was 1 MHz and 0.6 W/cm^2. Mizushige (1999) reported comparison of different types of microbubble ultrasound contrast agent (sonicated albumin (A)-, SH-U508A (SH) - and dodecafluoropentane emulsion (DDFP)) for drug-mediated thrombolysis. A catheter-type transducer capable of US emission (10 MHz, spatial peak temporal average intensity 1.02 W/cm^2 and peak negative pressure 0.33 MPa) in the continuous-wave mode was employed in artificial white thrombi. Serial changes in acoustic properties monitored by echography showed greatest reduction of the thrombus in the DDFP, and that in the sonicated albumin microbubble was not significantly different from controls. The stability of the microbubbles was an important factor for the difference. Culp (2004) conducted a transcranial ultrasound experiment in swine (1MHz, 2.0W/cm^2) in combination with platelet-targeted microbubbles and obtained rapid opening of intracranial thrombotic occlusions. Based on these results, ImaRx Therapeutics, Inc. (Arizona, USA) recently announced initiation of a multicenter Phase II clinical trial with a 40-patient, randomized and blinded study. This will evaluate the safety and effectiveness of thrombolysis with nanosized bubbles and ultrasound for the treatment of acute ischemic stroke without the use of lytic drugs. A result if microbubble alone could breakup thrombus in the middle cereberal artery from this trial is anticipated. Other applications in a range of thrombus related conditions including myocardial infarction, deep vein thrombosis and thrombi in dialysis grafts are also under consideration.

Another aspect which cannot be ignored is the possibility of using microbubbles to carry various drugs to target sites and rupturing the microbubbles by localized ultrasound energy. At moderately high sound pressure amplitudes at the acoustic pressure waves can cause the shells of coated microbubbles to rupture, freeing the bubbles so that they behave as non-coated microbubbles until they diffuse into the bloodstream. Drug-filled or drug-coated microspheres carrying a therapeutic compound may be targeted to specific tissues through the use of sonic energy, which is directed to the target area and causes the microspheres to rupture and release the therapeutic compound. Targeted drug delivery methods are particularly important where the toxicity of the drug is an issue. Specific drug delivery methods potentially serve to minimize toxic side effects, lower the required dosage amounts, and decrease costs for the patient. The most exciting application of this method is probably gene therapy. The methods and materials in the prior technology for introduction of genetic materials to, for example, living cells are limited and ineffective. Better means of delivery for therapeutics such as genetic materials are needed to treat a wide variety of diseases. Great strides have been made in characterizing genetic diseases and in understanding protein transcription, but relatively little progress has been made in delivering genetic material to cells for treatment. To date, several different mechanisms have been developed to deliver genetic material. These delivery mechanisms include techniques such as calcium phosphate precipitation and electroporation, and carriers such as cationic polymers and aqueous-filled liposomes. These methods have all been relatively ineffective in vivo and only of limited use for cell culture transfection. A principal difficulty has been to deliver the

genetic material from the extracellular space to the intracellular space or even to effectively localize genetic material at the surface of selected cell membranes. Viruses such as adenoviruses and retroviruses have been used as vectors to transfer genetic material to cells. However, it has also been difficult to develop a successfully targeted viral-mediated vector for delivery of genetic material in vivo.

Instead of viral vectors as the carrier of genes to targeted locations, pure plasmid DNA can be attached either to the outside or inside of the microbubble capsule wall. Bubbles can be collapsed by extracorporeal ultrasound or by intravascular ultrasound catheter, permitting the DNA to penetrate directly into the tissue and cells. Greenleaf (1997) demonstrated an increase in the transfection rate of DNA in the presence of albumin microbubbles in vitro. Unger et al (1997) demonstrated similar results with microbubble liposomes. Porter (2001) succeeded in reducing restenosis by antisense to the c-myc protooncogene bound to perflurocarbon microbubbles in pigs. Ultrasound may become a new, effective and safe means for introducing genetic material into the target cells of tissues. Although the exact mechanism is still unknown, it is believed that microspheres, upon rupture, create a local increase in membrane fluidity, thereby enhancing cellular uptake of the therapeutic compound (Ogawa 2001). There have been reports that differences in the gene transfer rate depended on the type of microbubbles similar to results from the thrombolysis (Tachibana 2003) however it is clear that gene delivery phenomenon occurs at a far smaller scale, thus further investigation is needed to understand the exact mechanism involved in ultrasound microbubble gene transfer. Recent observation of the collapse of microbubbles by the newly developed high speed video microscope Brandalis-128 system which has an average speed of 13 million frames per second has produced massive information on the dynamic behavior of ultrasound insonified encapsulated microbubbles (Postema 2004). Understanding more on the physics involved in the event of microjet in the following few years will perhaps solve how exactly genes penetrate the cell membrane (Marmottant 2003, 2004).

Regenerative Medicine

The concept of applying ultrasound as a means to alter the pharmacokinetics of drugs in various tissues has expanded into a whole new field beyond just drug delivery. Application of ultrasound for regenerative medicine is one of them. With the progress in gene therapy, ultrasound may become a new, effective and safe means for introducing genetic material into the target cells of tissues. Ultrasound can induce cell-membrane porosity (Tachibana 1999), and enhance the delivery of naked plasmid DNA into cells in vitro. Moreover, recent studies have shown enhanced permeability of naked plasmid DNA into tumors in vivo (Manome 2000) and Li (2003) recently made a comparison of gene transfection using various microbubbles available in the market. Ogawa (2002) also made comparison with different dissolved gases and found a change in the extent of gene transfection. Although the exact mechanism is still unknown, it is believed that microspheres, upon rupture, create a local increase in membrane fluidity, thereby enhancing cellular uptake of the therapeutic compound. "Sonoporation" as this phenomenon is frequently called is a new means to overcome limitations of other gene transduction methods. Nevertheless, different genes for various purposes are now under intensive investigation for possible use in regenerative medicine. This could be for angiogenesis, anti-angiogenesis, apoptosis, bone generation and other future treatments methods. Anti-sense oligodeoxynucleotides (AS-ODNs) have been recognized as a new generation of putative therapeutic agents,

Miura et al. 2002 established a delivery technique that could transfect AS-ODNs, which are designed for endothelin type B receptor (ETB), into cultured human coronary endothelial cells (HCECs) by exposure to ultrasound in the presence of echo contrast microbubbles. Taniyama (2002) has successfully transfected genes (HGF) for angiogenesis by ultrasound/microbubbles in skeletal muscles. This could lead to a cure for critical limb ischemia. In addition, Taniyama (2003) transfected an anti-oncogene (p53) plasmid into carotid artery after a balloon injury as a model of gene therapy for restenosis. Bone morphogenetic proteins (BMPs) are morphogens implicated both in embryonic and regenerative odontogenic differentiation. Gene therapy has the potential to improve induction of reparative dentin formation or potent bioactive pulp capping. Nakashima (2003) optimized the gene transfer of Growth/differentiation factor 11 (Gdf11)/Bmp11 plasmid DNA into dental pulp stem cells by sonoporation in vivo. Dental pulp tissue treated with plasmid pEGFP or CMV-LacZ in 5-10% Optison and irradiated by ultrasound (1MHz, 0.5W/cm^2, 30 sec) showed significant high efficiency of gene transfer and high level of protein production selectively in the insonated region, within 300 μm under the amputated site of the pulp tissue. The Gdf11 cDNA plasmid transferred into dental pulp tissue by sonoporation in vitro induced the expression of Dentin sialoprotein (Dsp), a differentiation marker for odontoblasts. The transfection of Gdf11 by sonoporation stimulated the large amount of reparative dentin formation on the amputated dental pulp in canine teeth in vivo. These results suggest the possible use of BMPs employing ultrasound-mediated gene therapy for endodontic dental treatments. It is estimated that genes for regeneration tissues could someday become a realistic mode of treatment. Other genes that have potential function for therapy have been reported to increase tranfection rate by ultrasound and microbubbles (Taniyama 2004, 2005; Manome 2005).

Sonodynamic Therapy

As a physical method used for the treatment of leukemia and solid cancers, compared to radiotherapy and light irradiation, ultrasonic irradiation is superior in that the applied energy can be focused solely on the cancer tissues to be treated with little effect upon normal tissues, and is better than light irradiation in the degree of penetration. Umemura (1990) pioneered in the development of non-thermal ultrasound to activate a group of chemicals that were originally used as light activated chemicals for cancer therapy. This new ultrasound therapy has been termed as sonodynamic therapy. Ultrasonic waves are known to affect chemical actions; for example, irradiation of water causes a reaction to generate hydrogen peroxide. As a result, it was found that certain drugs, upon ultrasonic irradiation, create active oxygen such as superoxide radicals and singlet oxygen, and the active oxygen thus formed effectively destructs cancer tissues (Miyoshi 1995). The agents themselves have no antitumor activity and, very low in toxicity, exhibit antitumor activity only by the chemical action caused by ultrasonic irradiation. Thus, there is less significant risk of causing any systemic disorder. In addition, these drug act exclusively upon tumor tissues when combined with ultrasonic irradiation, with no adverse effect upon normal tissues. An important factor involved in ultrasound irradiation is the chemical reactions induced during the course of violent microbubble collapse. Short-lived free radicals can be created by ultrasound that could alter various compounds leading to cell killing (Yumita 2003). Sonoluminescence may also be related with the complex sonochemical or sonodynamic reactions. However, the exact mechanism related to cytotoxicity still remains to be solved. Acoustic cavitation can

chemically activate photosensitive drugs specifically bound to malignant cell membrane which could result in cell surface disruption (Uchida 1997). In recent experiments with Adult T cell leukemia cells were specifically killed by low intensity ultrasound of 0.3W/cm^2 in the presence of porfimer sodium (Tachibana 1997). Abe (2002) developed a strategy for the selective destruction of cancer cells by ultrasonic irradiation in the presence of an antibody-conjugated photosensitizer. A photoimmunoconjugate (PIC) was prepared between ATX-70, a photosensitizer of a gallium-porphyrin analogue, and F11-39, a high affinity monoclonal antibody (MAb) against carcinoembryonic antigen (CEA), which is often overexpressed in various carcinoma cells. The conjugate, designated F39/ATX-70, retained immunoreactivity against purified CEA and CEA-expressing cells as determined by enzyme-linked immunosorbent assay, flow cytometry and immunofluorescence microscopic analysis. The cytotoxicity of F39/ATX-70 against CEA-expressing human gastric carcinoma cells in vitro was found to be greater than that of ATX-70 when applied in combination with ultrasound irradiation. In vivo anti-tumor effects in a mouse xenograft model resulted in a marked growth inhibition of tumor compared with ultrasound alone or ultrasound after administration of ATX-70. Arakawa (2002) demonstrated if PAD-S31, a water-soluble, chlorine-derivative sonochemical sensitizer, can be used for sonodynamic therapy on neointimal hyperplasia in a rabbit stent model. One hour after the intravenous administration of PAD-S31, ultrasound energy (1 MHz, 0.3 W/cm^2) was delivered transdermally to the sonodynamic therapy group. At 28 days, all stent sites were analyzed morphometrically. The ratio of the intimal and medial cross-sectional area was smaller in the sonodynamic therapy group than in the control, ultrasound, and PAD-S31 groups. It was concluded that sonodynamic therapy might be a feasible treatment modality for noninvasively inhibiting neointimal hyperplasia.

Anti-angiogenesis therapy is considered to be a new approach to various human cancers because angiogenesis is crucial for tumor growth (Emoto 2003). Moreover, ultrasound energy has been shown to enhance an anti-tumor effect of a chemotherapeutic agent in vitro and in vivo. Uterine sarcoma is the most malignant neoplasm among the known uterine malignancies, which has a poor response to any chemotherapeutic agent currently used and also radiotherapy. Our previous study showed anti-tumor effect of TNP-470 (an analogue of fumagillin), an angiogenesis inhibitor, for human uterine sarcoma, in vitro and in vivo. This study firstly examined the therapeutic effect of angiogenesis inhibitor combined with ultrasound irradiation for human cancer in vivo and evaluated its vascularity on real-time using a microbubble ultrasound contrast agent (Optison®). The uterine sarcoma xenografts were treated by ultrasound with an intensity of 2.0 w/cm^2, 1MHz for 4 min three times per week each after subcutaneous injection of TNP-470 at a dose of 30 mg/kg and this therapy was continued for eight weeks. It was found effective and with no major side effects. These results suggest that there is an accelerated (boosting) effect of ultrasound for anti-angiogenesis drug therapy for human uterine sarcoma and this combination therapy might be a potential candidate for a new cancer treatment

Feril (2003, 2005) recently reported monocytic leukemia cells (U937) killing effect by combining thermal-sensitive drug, 2, 2'-azobis (2-amidinopropane) dihydrochloride (AAPH) and exposure to nonthermal 1 MHz US for 1 min at intensity of 2.0 W/cm^2. Apoptosis measured by flow cytometry and free radical investigation using electron paramagnetic resonance (EPR) spin trapping

showed that US-induced cell lysis and apoptosis were enhanced in the presence of AAPH regardless of the temperature at the time of sonication. Although free radicals were increased in the combined treatment, this increase did not correlate well with cell killing. The mechanism of enhancement pointed to the increased uptake of the agent during sonication rather than potentiation by AAPH. Although much more research is needed to transfer experimental information to actual clinical cases, rapid advancement of HIFU will act as accelerating factor for future therapeutic strategies as combining anti-cancer drug and ultrasound in patients.

Conclusions and Outlook

Research on the bioeffects of ultrasound alone and in the presence of various drugs to the patients has only just begun. Most investigations are still on experimental level and far from being applicable in the clinical situation; however, such application as HIFU therapy for prostate cancer is already beginning to be widely used for patients as an alternative non-operative modality. Additionally, there definitely exists an interesting biological phenomenon that cannot be ignored when non-thermal ultrasound is applied. The interaction between ultrasound and drugs can range from a change in permeability of biological membrane to the manipulation of DNA into the cells. Recent discoveries have triggered the imagination of researchers in regenerative medicine and developmental research. Understanding the mechanism of micro/nano bubble collapse will eventually result in optimization of the acoustics and the design of ultrasound devices for wider clinical therapeutic applications and research.

Acknowledgments

This review was supported in part by a Grant-in-Aid for Scientific Research on Priority Areas (15300187, 16500328) from the Ministry of Education, Culture, Sports, Science and Technology, Japan and from Fukuoka University Central Research Institute.

References

Abe H, Kuroki M, Tachibana K, Li T, Awasthi A, Ueno A, Matsumoto H, Imakiire T, Yamauchi Y, Yamada H, Ariyoshi A, Kuroki M. Anticancer Res. 2002 May-Jun;22(3):1575-80.

Alexandrov AV, Demchuk AM, Hill MD. Stroke 2002; 33: 354-55.

Arakawa K, Hagisawa K, Kusano H, Yoneyama S, Kurita A, Arai T, Kikuchi M, Sakata I, Umenura Si S, Ohsuzu F. Circulation. 2002 Jan 15;105(2):149-51.

Bao S, Thrall BD, Miller DL. Ultrasound Med Biol. 1997;23(6):953-9.

Blinc A, Francis CW, Trudnowski JL, Carstensen EL. Blood. 1993 May 15;81(10):2636-43

Culp WC, Porter TR, Lowery J, Xie F, Roberson PK, Marky L Stroke. 2004 Oct;35(10):2407-11.

Emoto M, Ishiguro M, Iwasaki H, Kikuchi M, Kawarabayashi T. Gynecol Oncol. 2003 Apr;89(1):88-94.

Feril LB Jr, Kondo T, Zhao QL, Ogawa R, Tachibana K, Kudo N, Fujimoto S, Nakamura S. Ultrasound Med Biol. 2003 Feb;29(2):331-7.

Feril LB Jr, Ogawa R, Kobayashi H, Kikuchi H, Kondo T. Ultrason Sonochem. 2005 Aug;12(6):489-93.

Francis CW, Onundarson PT, Carstensen EL, Blinc A, Meltzer RS, Schwarz K, Marder VJ. J Clin Invest. 1992 Nov;90(5):2063-8.

Greenleaf WJ, Bolander ME, Sarkar G, Goldring MB, Greenleaf JF. Ultrasound Med Biol. 1998 May;24(4):587-95.

Ishibashi T, Akiyama M, Onoue H, Abe T, Furuhata H. Stroke. 2002 May;33(5):1399-404.

Kimura M, Iijima S, Kobayashi K, Furuhata H. Biol Pharm Bull. 1994 Jan;17(1):126-30.
Li T, Tachibana K, Kuroki M, Kuroki M. Radiology. 2003 Nov;229(2):423-8.
Mahon BR, Nesbit GM, Barnwell SL, Clark W, Marotta TR, Weill A, Teal PA, Qureshi A. AJNR Am J Neuroradiol. 2003 Mar;24(3):534-8.
Manome Y, Nakamura M, Ohno T, Furuhata H. Hum Gene Ther. 2000 Jul 20;11(11):1521-8
Manome Y, Nakayama N, Nakayama K, Furuhata H. Ultrasound Med Biol. 2005 May;31(5):693-702.
Marmottant P, Hilgenfeldt S. Nature. 2003 May 8;423(6936):153-6.
Marmottant P, Hilgenfeldt S Proc Natl Acad Sci U S A. 2004 Jun 29;101(26):9523-7.
Miura S, Tachibana K, Okamoto T, Saku K. Biochem Biophys Res Commun. 2002 Nov 8;298(4):587-90.
Miyoshi N, Misik V, Fukuda M, Riesz P. Radiat Res. 1995 Aug;143(2):194-202.
Mizushige K, Kondo I, Ohmori K, Hirao K, Matsuo H. Ultrasound Med Biol. 1999 Nov;25(9):1431-7.
Nakashima M, Tachibana K, Iohara K, Ito M, Ishikawa M, Akamine A. Hum Gene Ther. 2003 Apr 10;14(6):591-7.
Ogawa K, Tachibana K, Uchida T, Tai T, Yamashita N, Tsujita N, Miyauchi R. Med Electron Microsc. 2001 Dec;34(4):249-53.
Ogawa R, Kondo T, Honda H, Zhao QL, Fukuda S, Riesz P. Ultrason Sonochem. 2002 Sep;9(4):197-203.
Porter TR, LeVeen RF, Fox R, Kricsfeld A, Xie F. Am Heart J. 1996 Nov;132(5):964-8.
Porter TR, Hiser WL, Kricsfeld D, Deligonul U, Xie F, Iversen P, Radio S. Ultrasound Med Biol. 2001 Feb;27(2):259-65.
Postema M, van Wamel A, Lancee CT, de Jong N. Ultrasound Med Biol. 2004 Jun;30(6):827-40.
Tachiban K, Kuroki M, Kuroki M. Radiology. 2003 229 (2): 423-8.
Tachibana S, Koga E. Blood and Vessel. 1981; 12: 450-53.
Tachibana K, Tachibana S. J Pharm Pharmacol. 1991 Apr;43(4):270-1.
Tachibana K. J Vasc Interv Radiol. 1992 May;3(2):299-303.
Tachibana K. Pharm Res. 1992 Jul;9(7):952-4.
Tachibana K, Tachibana S. Circulation 1995; 92: 1148-1150
Tachibana K, Uchida T, Hisano S, Morioka E. Lancet. 1997 Feb 1;349(9048):325.
Tachibana K, Uchida T, Ogawa K, Yamashita N, Tamura K. Lancet. 1999 Apr 24;353(9162):1409.
Taniyama Y, Tachibana K, Hiraoka K, Aoki M, Yamamoto S, Matsumoto K, Nakamura T, Ogihara T, Kaneda Y, Morishita R. Gene Ther. 2002 Mar;9(6):372-80.
Taniyama Y, Tachibana K, Hiraoka K, Namba T, Yamasaki K, Hashiya N, Aoki M, Ogihara T, Yasufumi K, Morishita R. Circulation. 2002 Mar 12;105(10):1233-9.
Uchida T, Tachibana K, Hisano S, Morioka E. Anticancer Drugs. 1997 Apr;8(4):329-35.
Unger EC, McCreery TP, Sweitzer RH. Invest Radiol. 1997 Dec;32(12):723-7.
Unger EC, Porter T, Culp W, Labell R, Matsunaga T, Zutshi R. Adv Drug Deliv Rev. 2004 May 7;56(9):1291-314.
Umemura S, Yumita N, Nishigaki R, Umemura K. Jpn J Cancer Res. 1990 Sep;81(9):962-6.
Ward M, Wu J, Chiu JF. J Acoust Soc Am. 1999 May;105(5):2951-7.
Yumita N, Sakata I, Nakajima S, Umemura S. Biochim Biophys Acta. 2003 Mar 17;1620(1-3):179-84.

ISSN 0117-150X

PHILIPPINE 2006 Physics Journal

volume 28

A publication of the Philippine Physics Society committed to the advancement of physics and physics education in the Philippines, especially in the Visayas and Mindanao and underserved areas in Luzon

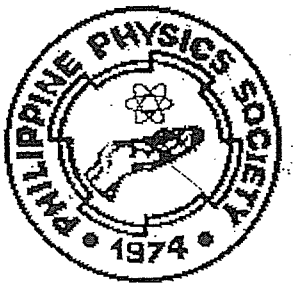

Gene Transfer to Corneal Epithelium and Keratocytes Mediated by Ultrasound with Microbubbles

Shozo Sonoda,[1] Katsuro Tachibana,[2] Eisuke Uchino,[1] Akiko Okubo,[1] Matsuo Yamamoto,[3] Kenji Sakoda,[4] Toshio Hisatomi,[5] Koh-Hei Sonoda,[5] Yoichi Negishi,[6] Yuichi Izumi,[4] Sonshin Takao,[7] and Taiji Sakamoto[1]

PURPOSE. The cornea is an ideal organ for evaluating gene transfer because it can be treated noninvasively and monitored easily. The present study was performed to investigate the practical efficacy and safety of ultrasound (US) plus microbubble (MB)–mediated gene transfer to cornea.

METHODS. Cultured rabbit corneal epithelial (RC-1) cells were incubated in 24-well dishes with plasmid DNA having a green fluorescent protein (GFP) gene under a cytomegalovirus promoter. The cells were exposed to US under different intensities (1 MHz; power, 0.5~2 W/cm^2; duration, 15–120 seconds; duty cycle, 20%–100%). The effect of simultaneous stimulation with MBs was also examined. Gene transfer was quantified by counting the number of GFP-positive cells under microscopy. Furthermore, in vivo gene transfer was examined by GFP plasmid injection into rabbit cornea and US exposure with MBs.

RESULTS. In the in vitro study, DNA exposure alone could not transfer gene into cultured RC-1 cells; US enhanced gene transfer slightly. Coexposure with MBs significantly increased gene transfer efficiency. In the in vivo study, DNA injection alone could transfer the gene to a limited degree, but plasmid injection plus US with MBs strongly increased gene transfer efficiency without apparent tissue damage, and gene transfer was achieved two dimensionally.

CONCLUSIONS. US with MBs greatly increases gene transfer to in vivo and in vitro corneal cells. This noninvasive gene transfer method may be a useful tool for clinical gene therapy. (*Invest Ophthalmol Vis Sci.* 2006;47:558–564) DOI:10.1167/iovs.05-0889

A modality to efficiently deliver genes to living tissue is essential for gene therapy and genetic research. The basic technology of gene delivery can be divided into two categories, a virus vector–mediated method and a non-virus vector–mediated method.[1–3] The virus vector–mediated method can transfer the gene of interest with high efficiency, but concern about safety issues prevents clinical application for common diseases.[3–5] The non-virus vector–mediated method is comparatively safe, but gene transfer efficiency does not reach a satisfactory level.[6–9] Among these methods, the mechanical enhancing method is unique because it is free from a biochemical agent that has not been proven to be safe for humans; thus, clinical application might be more easily accepted. Electroporation can be used for this purpose but often results in severe cell damage.[10,11] In contrast, it recently became apparent that ultrasound (US) can enhance gene transfer to mammalian cells in vitro and in vivo without cell damage,[12–16] and US-mediated gene therapy has been reported in vessels and muscles of animal studies.[17,18] US is now widely used for clinical examinations and therapies, and its safety has been reliably established.

The cornea plays an important role in maintaining vision. Vision can be seriously impaired as a result of corneal cloudiness caused by insufficient wound healing or by the metabolic processes of cornea. Although corneal surgery is widely performed and may be performed even more often as more refractive surgery is performed, the cellular and molecular events that control wound healing within the corneal stroma are not well understood.[19,20] The cornea is an external tissue suitable for gene therapy because of its easy accessibility by surgical maneuvers, including US. In addition, gene transfer can be easily monitored by noninvasive methods such as microscopic observation.[21]

Microbubbles (MBs), which are gas bubbles measuring approximately 3 μm in diameter, have been developed mainly as contrast agents to improve ultrasonographic images. They have shown promise in gene therapy for several reasons. MBs act as cavitation nuclei, effectively focusing ultrasound energy, and they can potentiate bioeffects. Evidence indicates that the ultrasound energy needed can be greatly reduced; therefore, the lower power used in diagnostic imaging systems may be sufficient to produce therapeutic effects.[22–24]

Simultaneous use of US and MBs has been found to increase gene transfer efficiency.[25–32] However, to our knowledge, few reports have been published of detailed analyses of US-mediated gene transfer with MBs. In this study, we performed a detailed analysis of gene transfer mediated by US with MBs using cornea, and we show two-dimensional gene transfer achieved by this method.

METHODS

In Vitro Study

Cell Culture. Rabbit corneal epithelial (RC-1) cells (JCRB0246) were obtained from Human Science Research Resource Bank (Tokyo, Japan) and incubated in modified Eagles medium (MEM; Sigma-Aldrich, St. Louis, MO) with 10% fetal bovine serum (FBS; Invitrogen-Gibco, Grand Island, NY) and streptomycin/penicillin (Wako, Osaka, Japan). All cells used in the studies were from passages 4 to 6.

From the Departments of [1]Ophthalmology and [4]Periodontology and the [7]Research Center for Life Science Resources, Kagoshima University, Kagoshima, Japan; the [2]Department of Anatomy, Fukuoka University School of Medicine, Fukuoka, Japan; the [3]Department of Periodontology, Showa University School of Dentistry, Tokyo, Japan; the [5]Department of Ophthalmology, Graduate School of Medical Sciences, Kyushu University, Fukuoka, Japan; and the [6]School of Pharmacy, Tokyo University of Pharmacy and Life Sciences, Tokyo, Japan.

Supported by Grants-in-Aid for Scientific Research (17390469 and 14370560) and Grant-in-Aid for Young Scientists (16791056) from the Ministry of Education, Science and Culture of the Japanese Government.

Submitted for publication July 11, 2005; revised September 9, 2005; accepted December 22, 2005.

Disclosure: **S. Sonoda**, None; **K. Tachibana**, None; **E. Uchino**, None; **A. Okubo**, None; **M. Yamamoto**, None; **K. Sakoda**, None; **T. Hisatomi**, None; **K.-H. Sonoda**, None; **Y. Negishi**, None; **Y. Izumi**, None; **S. Takao**, None; **T. Sakamoto**, None

The publication costs of this article were defrayed in part by page charge payment. This article must therefore be marked "*advertisement*" in accordance with 18 U.S.C. §1734 solely to indicate this fact.

Corresponding author: Taiji Sakamoto, Department of Ophthalmology, Kagoshima University Faculty of Medicine, 8-35-1 Sakuragaoka, Kagoshima, Japan 890-8520; tsakamot@m3.kufm.kagoshima-u.ac.jp.

Investigative Ophthalmology & Visual Science, February 2006, Vol. 47, No. 2

Plasmids. An expression vector for the green fluorescent protein (GFP) gene, *pEGFP-N2*, a mammalian expression vector containing a cytomegalovirus immediate-early enhancer/promoter, was obtained from Clontech Co., Ltd. (Palo Alto, CA). Plasmids grown in *Escherichia coli* host strain XLI-blue were purified (Plasmid Kit; Qiagen, Valencia, CA) and suspended in TE buffer (pH 8.0) at a concentration of 1.0 μg/μL. Plasmids were then suspended in phosphate-buffered saline (PBS; Invitrogen-Gibco), and the pH was adjusted to 7.35.

Ultrasound Exposure. RC-1 cells were collected with trypsin (Sigma-Aldrich), passed through a cell strainer (Becton Dickinson, Franklin Lakes, NJ), and put into a 48-well collagen type 1–coated glass bottom chamber (Asahi Technoglass, Chiba, Japan) filled with 400 μL MEM with 10% FBS, 4×10^4 cells/well. A plasmid solution 0.5 μL was added to the medium. Immediately thereafter, US was exposed to the medium using a 6-mm probe generated by an US machine (Sonitron 2000; Richmar, Inola, OK). During exposure, the medium-containing cells were gently stirred by a magnetic stirrer (300 rpm). To induce MBs, perflutren protein type A microsphere (Optison; Amersham Health, Princeton, NJ)—a well-established, second-generation US medical diagnostic product with robust capability—was used. It is an albumin-shelled US contrast agent composed of approximately $5 \text{ to } 8 \times 10^8$ MBs per milliliter measuring between 2 and 4.5 μm in diameter and filled with octaperfluoropropane. The indicated percentage was added to the plasmid solution (0.5, 0.25, or 0.1 μL), gently mixed, and left for 60 seconds. Immediately thereafter, the mixed solution was added to the dish and exposed to US as described.

Gene Transfer Efficiency. After gene transfer treatment, including plasmid alone or plasmid plus US exposure, the cells were incubated in a medium containing 10% FBS for 48 hours and then were observed by phase-contrast microscopy with or without a 515-nm filter (Olympus, Tokyo, Japan). A randomly selected field (4 fields/well with 100 × magnification) was photographed. The photographs were monitored by a NIH image analyzer, and the ratio of GFP-positive cells to all cells in each field was evaluated by masked observers. To determine the duration of GFP expression, GFP expression was evaluated on days 4, 8, 14, and 30.

Cell Survival and Cell Damage. Survival of cells was evaluated by counting living cells. Briefly, after 48 hours of incubation, the dishes were washed twice with PBS, four microscopic fields per well were photographed, and the living cells were counted. Cell damage was evaluated by lactate dehydrogenase (LDH)–releasing assay according as the manufacturer's instructions (Roche, Penzberg, Germany). Cells cultured on a 48-well plate were treated by each procedure, and cell damage was evaluated after 6 hours. The most severe cell damage was obtained by treatment with 1% Triton X (Sigma-Aldrich) and was used as a positive control. Cells with no treatment were applied as negative controls. Cell damage was expressed as: % LDH of sample − LDH of negative control/LDH of positive control − LDH of negative control.

In Vivo Study

After obtaining the approval of Kagoshima University ethics committee, all animals were used humanely in strict compliance with the ARVO Statement for the Use of Animals in Ophthalmic and Vision Research.

New Zealand albino rabbits (male; age, 14 weeks; weight, 3000 g; KBT Oriental Co., Saga, Japan) were first anesthetized with intramuscular injection of ketamine hydrochloride (14 mg/kg) and xylazine hydrochloride (14 mg/kg). Plasmid 10 μL mixed with PBS 2 μL was injected under surgical microscopy into the center of each cornea using a syringe with a 30-gauge needle. Immediately thereafter, a 6-mm US probe was placed directly on the corneal surface, and US was generated. When MBs were used, plasmid 10 μL mixed with perflutren protein (Optison; Amersham Health) 2 μL was injected instead of a plasmid with PBS. The intensity of US was set at 1 MHz, 120 seconds, 50% duty cycle, and 3 US powers—1 W/cm², 1.5 W/cm², and 2 W/cm²—were examined.

GFP Expression. The presence of fluorescence signaling in the in vivo gene expression was determined using direct stereomicroscopy 72 hours after gene transfer (Olympus, Tokyo, Japan). The value of gene transfer was graded according to our scoring system by 3 masked observers. Only GFP expression scores agreed to by at least 2 of the observers were used in the analysis. Scoring criteria and representative photographs are shown in Figure 1. Transfection efficiency was expressed by a score of 0 to 5 (0 = not GFP positive; 5 = most intensely GFP positive).

Histology. All the animals were killed by overdose intravenous injection of pentobarbital. The eyes were enucleated 48 hours after treatment and were immediately frozen in liquid N2–cooled isopentane. Serial sections (6 μm) were sliced with a cryostat, placed on slides, and air dried. Regular fluorescent images and differential interference images were obtained by fluorescence microscopy (BX-FLA; Olympus, Tokyo, Japan) and were fitted using the IP Laboratory program (Scanalytics, Inc.; Fairfax, VA) on a personal computer. For light microscopy, the eyes were fixed with 3.7% formaldehyde in PBS, dehydrated with a graded alcohol series, and embedded in paraffin. Sections were cut and stained with hematoxylin and eosin. For the electron microscopy, the tissue was fixed with 4% paraformaldehyde, and the specimens were then dehydrated in a series of graded ethanols and embedded in epoxy resin. Thin sections were cut on an ultramicrotome, stained with uranyl acetate–lead citrate, and observed with an electron microscope (JEM-100CX; JEOL, Tokyo, Japan), as described. All the specimens were then observed by 2 masked observers who received no information about the specimens.

FIGURE 1. Representative photographs of scoring criteria. Gene transfer efficiency was expressed as a score of 0 to 5. Scoring was performed by 3 masked observers according to the following criteria. 0: no positive cells; 1: 1 to 25 positive cells in each field; 2: 26 to 50 positive cells in each field; 3: 51 to 75 positive cells in each field; 4: 75 to 150 positive cells in each field; 5: 151 or more positive cells in each field. Bar, 400 μm.

Statistical Analysis

All values were expressed as mean ± SEM. Analysis of variance with subsequent Scheffe test and Mann-Whitney *U* test was used to determine the significance of the difference in multiple comparison. Differences with a $P < 0.05$ were considered significant.

Results

In Vitro Study

Gene Transfer by Ultrasound. Numerous RC-1 cells were GFP positive after US exposure with the plasmid solution (Fig. 2A). Cells treated with the plasmid solution alone or the plasmid solution with MB perflutren protein (Optison; Amersham Health) alone did not show any fluorescein (Fig. 2B).

Gene Transfer by US Plus MBs. Under any of the following experimental US conditions—1 W/cm^2, 60 seconds, duty cycle 50%; 1 W/cm^2, 120 seconds, duty cycle 50%; 2 W/cm^2, 60 seconds, duty cycle 50%; 2 W/cm^2, 120 seconds, duty cycle 50%—the ratio of GFP-positive cells treated by US with MBs was significantly (two to four times) higher than that by US alone (Mann-Whitney *U* test, $P < 0.01$ Fig. 2C). To identify the optimal conditions to transfer genes by US plus MBs, the following four parameters were examined.

Duty Cycle. According to our previous studies, three duty cycles (20%, 50%, or 100%) were examined under an intensity of 1 W/cm^2 and 60-second exposure with 20% MBs.[29,30,32] As a result, the GFP-positive cell ratios were 11.3% with a duty cycle of 20%, 18.0% with a duty cycle of 50%, and 35.6% with a duty cycle of 100%. The GFP-positive cell ratio of duty cycle 100% US plus MBs was significantly higher than that under the other three conditions (Scheffe test, $P < 0.01$; Fig. 3A). On the other hand, the average number of survival cells was low with a duty cycle of 100%; for 79 cells per field, the duty cycle was 20%; for 171 cells per field, it was 50%; for 17.1 cells per field per, it was 100%. Cell damage was high in US, with a duty cycle of 20% or 100% in LDH assay (Fig. 3B). These results indicate that a duty cycle of 50% is preferable for obtaining high gene transfer efficiency with minimal cell damage.

MBs. Three concentrations of MBs—20%, 50%, and 100%—were examined under the US condition of 1 W/cm^2, 60 seconds, and duty cycle 50%. The GFP-positive ratio was highest in cells treated by US with 20% MBs (Scheffe test, $P < 0.01$; Fig. 3C). Cell survival was lowest in the 100% MB group, and no significant difference was found between the 20% and the 50% MB groups (170.7 cells/field in 20% MBs, 163 cells/field in 50% MBs, 38 cells/field in 100% MBs). A similar tendency was found by LDH assay (data not shown). Thus, 20% MBs was preferable.

Exposure Time. According to our previous study, a US exposure duration exceeding 120 seconds significantly damaged cells[29,32]; thus, a US exposure time of 15 to 120 seconds was examined under the condition of 1 W/cm^2, duty cycle 50%, with 20% MBs. As a result, the GFP-positive ratio was equally high for 60-and 120-second exposures (Fig. 3D). Cell damage was not apparent in any experimental group (Fig. 3E).

US Intensity. US intensities of 0.5, 1.0, 1.5, and 2.0 W/cm^2 were examined under the condition of 50% duty cycle and 60-second exposure with 20% MBs. A GFP-positive ratio of 0.5 W/cm^2 US group was significantly smaller than that in any of the other 3 groups (Scheffe test, $P < 0.01$; Fig. 2F). LDH assay also indicated that cell damage was significantly high in the 1.5 and 2.0 W/cm^2 exposure groups ($P < 0.01$; Fig. 3G), whereas little cell damage was observed in cells treated with 0.5 or 1.0 W/cm^2 US intensity. Representative images are shown in Figures 3H and 3I.

In Vivo Study

Gene Transfer by US. All GFP-positive cells in rabbit eyes underwent treatment. Eyes that received plasmid injection alone showed mild GFP-positive cells distributed within the injected area. GFP-positive cells were observed mainly in the corneal stroma. Average fluorescein score was 2.1 ($n = 24$). On the other hand, eyes that received plasmid injection and US (1 W/cm^2, 120 seconds, duty cycle 50%) had more GFP-positive cells (average score, 2.6; $n = 14$) than those that received plasmid injection alone. However, the difference was not statistically significant (Fig. 4).

Gene Transfer by US and MBs. From the in vitro study, 20% MBs were chosen. The average score of GFP-positive cells in cornea was 3.5 for eyes treated by US of 1 W/cm^2, 120 seconds, 50% duty cycle with MBs ($n = 41$). A significantly higher score (4.5) was obtained with simultaneous treatment by US and MBs than by US alone (2.6) or MBs alone (2.0) (Scheffe test, $P < 0.05$; Fig. 4), and it was achieved with US of 2 W/cm^2, 120 seconds, and 50% duty cycle ($n = 12$). GFP-

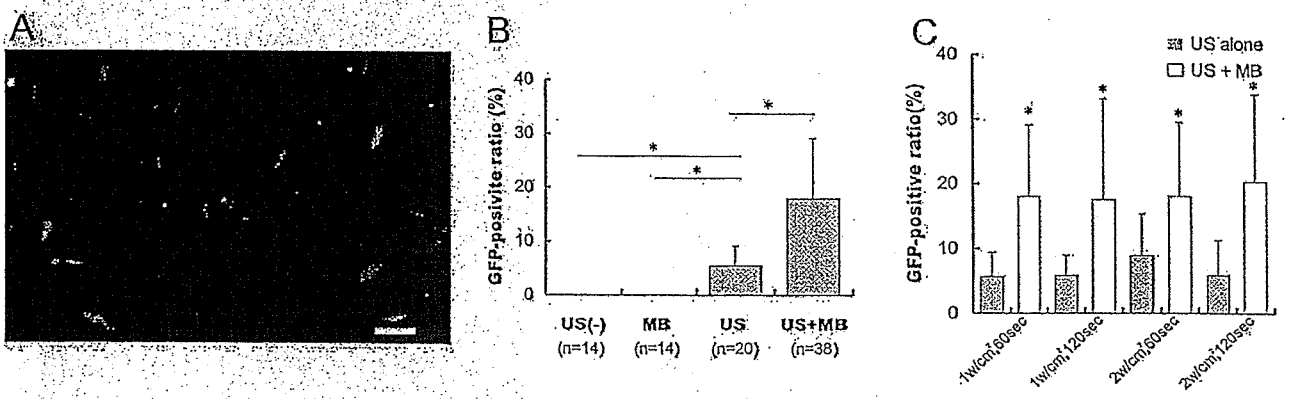

FIGURE 2. GFP-positive cells in gene-transferred rabbit corneal epithelial (RC-1) cells. (A) Fluorescence photograph of gene-transferred RC-1 cells. Many cells show a GFP-positive reaction in the whole cytoplasm. Bar, 100 μm. (B) GFP-positive ratio by different methods. Numerous RC-1 cells were GFP positive after ultrasonic exposure with the plasmid solution. Cells treated with the plasmid solution alone or the plasmid solution with perflutren protein (Optison; Amersham Health) alone did not show any fluorescein (Mann-Whitney *U* test, $^*P < 0.01$). (C) GFP-positive ratio of cells treated by US exposure with MBs. GFP-positive ratio treated by US with MBs was significantly higher (2–4 times) than that by US alone (Mann-Whitney *U* test, $^*P < 0.01$). 1 W/cm^2, 60 seconds, duty cycle 50%: US only, $n = 14$; with MB, $n = 38$. 1 W/cm^2, 120 seconds, duty cycle 50%: US only, $n = 15$; with MB, $n = 24$. 2 W/cm^2, 60 seconds, duty cycle 50%: US only, $n = 15$; with MB, $n = 23$. 2 W/cm^2, 120 seconds, duty cycle 50%: US only, $n = 15$; with MB, $n = 13$.

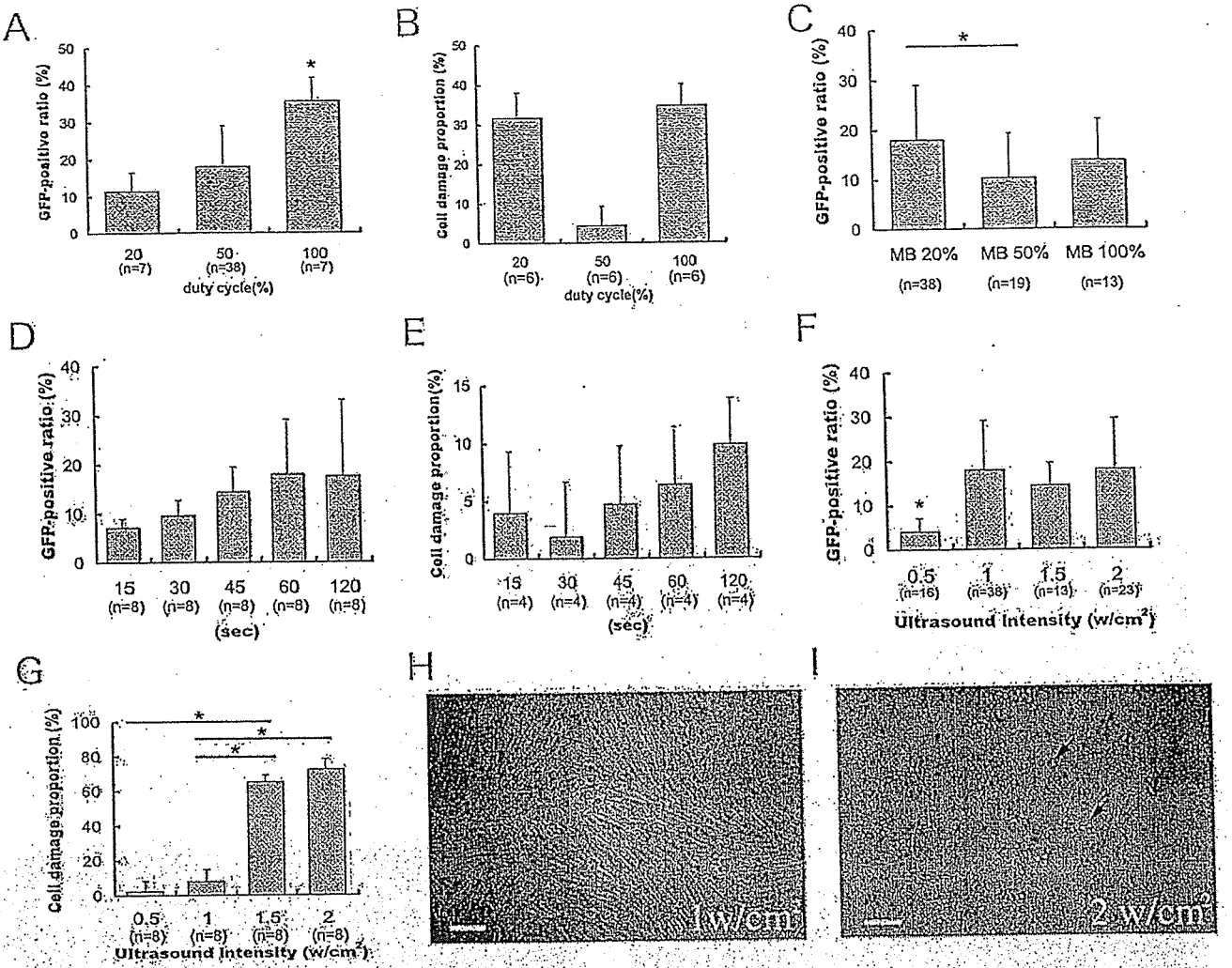

FIGURE 3. Gene transfer by US and MBs under different conditions. (A) GFP-positive ratio at a different duty cycle. GFP-positive ratio of duty cycle 100% US plus MBs was significantly higher than under the other 3 conditions (Scheffe test, $^*P < 0.01$). (B) Cell damage at different duty cycle. LDH assay indicates that cell damage was high in US at duty cycle 20% or 100%. (C) GFP-positive ratio at different concentrations of MBs. GFP-positive ratio was highest in cells treated by US with 20% MBs (Scheffe test, $^*P < 0.01$). (D) GFP-positive ratio at different US exposure times. GFP-positive ratio was equally high at 60- and 120-second exposures. (E) Cell damage at different US exposure times. Cell damage was not apparent in any experimental group. (F) GFP-positive ratio at different US powers. GFP-positive ratio of 0.5 W/cm^2 US group was significantly smaller than that of any of the other 3 groups (Scheffe test, $^*P < 0.01$). (G) Cell damage at different US powers. LDH assay indicates that cell damage was significantly high in the 1.5 or 2.0 W/cm^2 exposure group ($^*P < 0.01$), whereas little cell damage was noticed in cells treated with 0.5 or 1.0 W/cm^2 US power. (H) Phase-contrast photograph of RC-1 cells immediately after US exposure. No apparent cell damage was observed. Bar, 100 μm. (I) Phase-contrast photograph of RC-1 cells immediately after US exposure. Apparent cell damage was found in many cells (*arrows*). Bar, 100 μm.

positive cells were observed exclusively where US was exposed (Fig. 5). US intensity greater than 3 W/cm^2 caused immediate stromal haziness, which resolved spontaneously with no treatment (data not shown).

Duration of GFP Expression. The duration of GFP expression in cornea was evaluated in the eye treated with US and MBs under 20% MBs, 2 W/cm^2, 120 seconds, duty cycle 50%. GFP-positive cells appeared on the following day and increased the strength and the number of GFP-positive cells for 8 days (Fig. 6). GFP-positive cells in cornea gradually decreased in number and strength over time, and the average GFP-positive score on day 14 was 2 ($n = 13$) (Scheffe test $P < 0.01$). On day 30, only a faint GFP-positive reaction was noticed ($n = 4$).

Histologic Findings. Fluorescence microscopic examination showed that GFP was present in spindle-shaped cells in the targeted regions of the corneal stroma; thus, we speculated that keratocytes were also present (Fig. 7). Importantly GFP-positive cells were limited to the US-exposed area. No GFP was detected in untreated cornea or other intraocular tissues, such as ciliary epithelial cells, trabecular meshwork, cells lining Schlemm canal, lens epithelial cells, or retina (data not shown). Light and electron microscopic examination 48 hours after treatment showed no corneal damage, such as opacity or persistent epithelial defects, after US plus MB treatment, even under the strongest power studied in this series (2 W/cm^2, 120 seconds, duty cycle 100%; data not shown).

DISCUSSION

US is broadly used for clinical imaging, and its safety has been reliably established. Only in the past few years have studies demonstrated US-enhanced gene delivery to mammalian cells in vitro and in vivo.[12–18] Moreover, the presence of MBs near

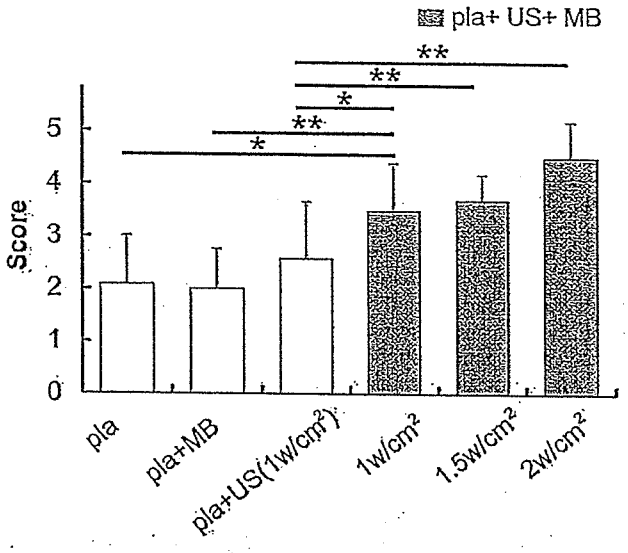

FIGURE 4. Gene transfer to rabbit cornea in vivo by US or MBs. Eyes that received plasmid injection alone or plasmid with MBs showed fluorescein-positive cells widely distributed within the injected area (plasmid alone, $n = 24$; plasmid with MB, $n = 8$). Eyes that received plasmid injection and US showed more numerous GFP-positive cells ($n = 14$) than those that received plasmid injection alone. A significantly higher score was obtained by simultaneous treatment of US and MBs (1 W/cm², $n = 41$; 1.5 W/cm², $n = 13$; 2 W/cm², $n = 12$) than by US alone (2.6) or MBs alone (2.0) (Scheffe test, $^*P < 0.05$, $^{**}P < 0.01$). Pla, plasmid DNA injection.

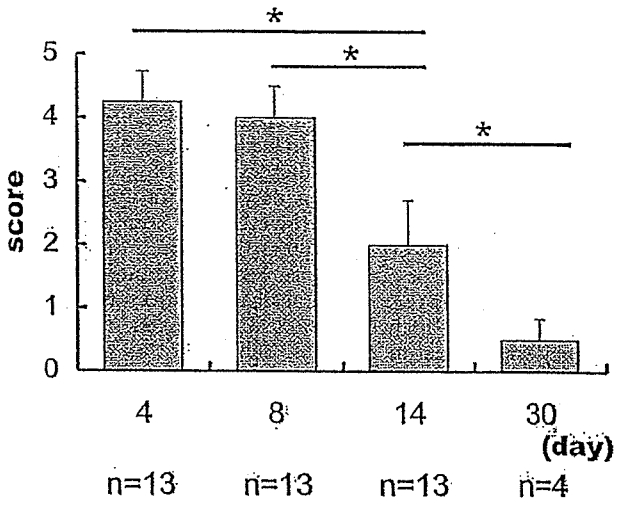

FIGURE 6. Duration of GFP expression in rabbit cornea was evaluated in the eye treated with US and MBs. GFP-positive cells appeared on the following day and increased the strength and number of GFP-positive cells for 8 days. GFP-positive cells in cornea gradually decreased in number and strength over time, and the average GFP-positive score on day 14 was 2 ($n = 13$) (Scheffe test, $^*P < 0.01$). On day 30, only faint GFP-positive reaction was observed ($n = 4$).

the cells further increases the gene transfection rate by lowering the acoustic pressure threshold needed to induce the microjets that penetrate the cellular membrane.[25–32] Sonography contrast-agent MBs with diameters ranging from 1 to 10 μm are considered ideal for this purpose. To gain further insight into the practicability of sonoporation, the cornea was selected as the subject of the present study because it can be noninvasively treated and monitored with the use of standard ophthalmological equipment, allowing visualization the cornea and the surrounding tissues under high magnification and per-

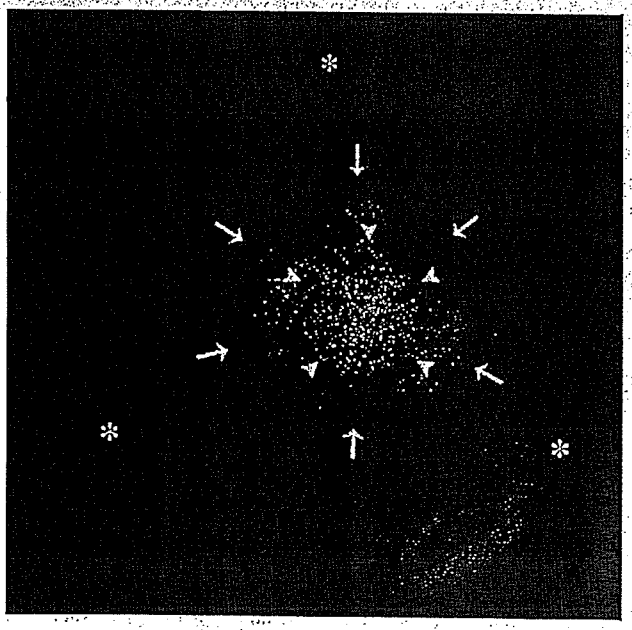

FIGURE 5. Fluorescence photograph of rabbit cornea 7 days after treatment. Twelve microliters plasmid with MBs was injected into the central cornea (*arrows*); this was followed by US exposure. *Arrowheads* indicate exactly where the US probe was placed. GFP-positive cells were specifically located where the US was exposed. A few GFP-positive cells are seen in the surrounding area. *Asterisks* indicate the corneal margin.

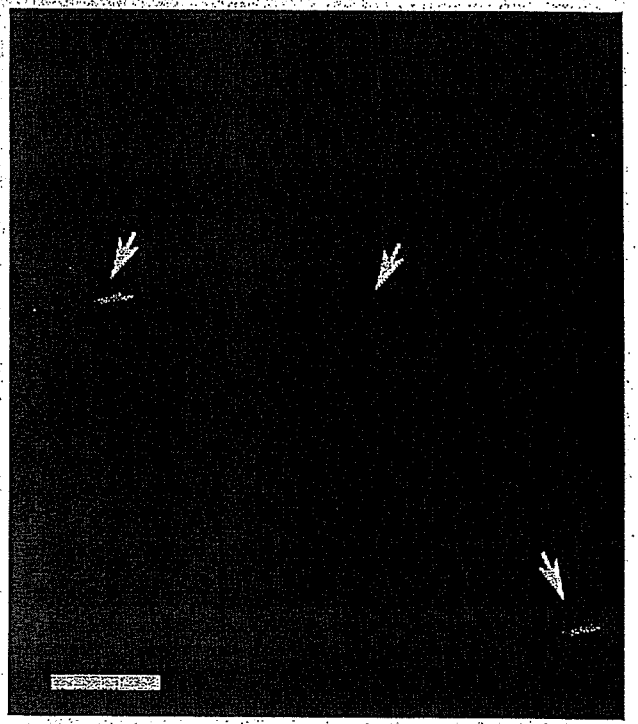

FIGURE 7. Fluorescence microscope photograph of rabbit cornea after treatment with US and MBs (2 W/cm², duty cycle 50%, 120 seconds). GFP is present mainly in spindle-shaped cells in the targeted regions of the corneal stroma (*arrows*). Bar, 10 μm.

mitting easy determination of gene transfection and tissue damage.

To establish the optimal condition of US MB–mediated gene transfer to cornea, 98 different patterns of various US conditions were examined in vitro in preliminary studies because it is difficult in practice to study so many different patterns using rabbit eyes in vivo. First, the duty cycle of US was evaluated. Results clearly showed that a duty cycle of 100% is most effective to transfer genes. However, cell damage was too strong with a duty cycle of 100%. Therefore, a duty cycle of 50% was chosen for our purpose. Second, the amount of MBs perflutren protein (Optison; Amersham Health) was evaluated. Cytotoxicity was highest in 100% MBs, and gene transfer efficiency was highest in 20% MBs. Thus, 20% MBs was chosen. Third, the exposure time of US was evaluated. An exposure time longer than 120 seconds significantly damaged the cells, and an exposure time shorter than 60 seconds could not transfer the gene efficiently. Sixty- and 120-second exposure provided almost identical gene transfer efficiency and cell toxicity. Finally, US power was studied. It is understandable that high US power can transfer the gene to cells but also induce strong cell damage. Considering gene transfer efficiency and cellular damage, a US power of 1 or 2 W/cm^2 should be appropriate.

Contrary to in vitro experiments, US alone revealed no significant enhancement of gene transfer compared with controls. Because the cornea is composed of multiple cell layers and abundant extracellular matrix, it is postulated that higher US intensities are needed to produce sufficient microjets to damage cells or inject genes into cells. Adding MB with the plasmids, on the other hand, increased gene transfer efficiency by twofold to threefold. Optic examination showed that GFP was present mainly in keratocytes at the US-targeted regions of the corneal stroma. GFP was not detected in the untreated area of the cornea or other intraocular tissues. It is noteworthy that US induced no immediate corneal damage, such as opacity or defect of corneal/ciliary epithelial cells. Surrounding trabecular meshwork, cells lining Schlemm canal, lens epithelial cells, and retina seemed to be intact.

Previously, Wang et al.[22] reported perflutren protein (Optison; Amersham Health) with DNA could achieve effective gene transfer in muscle. However, effective gene transfer could not be performed in cornea in the present study. Because the cornea has more abundant extracellular materials than muscle, perflutren protein (Optison; Amersham Health) alone might not be effective for transferring DNA to cells.

Viral vector– or liposome-mediated gene transfer methods are effective for transferring genes to almost every cell that comes in contact with vectors[33,34] (e.g., the adenoviral vector). Because the long-term effects of gene transfer on recipient cells remain unclear, the cells to which genes are transferred should be strictly controlled. Especially when transferring genes to the cornea, the pupillary area should be avoided so as not to threaten vision. The present method greatly reduces this concern because of the precise targeting it makes possible.

In previous studies we reported that electroporation-mediated gene transfer can be achieved in rat cornea.[35–37] However, in larger animals, including rabbit, electroporation may be hazardous because the cardiovascular system is sometimes impaired by treatment (data not shown). Therefore, at present it might not be easy to apply electroporation for human gene therapy.

When the vehicle with the gene of interest is injected into tissue through a local gene delivery method such as liposome or viral vector injection, the vehicle spreads in every direction three dimensionally. Accordingly, gene transfer is achieved three dimensionally in a similar way. However, in the treatment of a surface organ such as skin or cornea, two-dimensional gene transfer is sometimes preferable. Using the characteristics of ultrasound, the present method achieved two-dimensional gene transfer.

Thirty percent to 40% of the total corneal area was covered by a 12-μL plasmid injection. Gene transfer was achieved in the area exposed to US. To expand the area of gene transfer, it was necessary to improve the injection method and the US probe. The present method can be applied to a variety of purposes, such as making it feasible to use highly fragile proteins.[38,39] With the present method, we were able to superficially deliver genes to a targeted tissue surface area two dimensionally. Thus, this sonoporation method could become a valuable modality for therapy and research that require surface-localized drug delivery or gene induction.[40]

Many questions remain before the present method can be applied clinically. The optimal US condition required for efficient gene transfer is highly dependent on the tissue, and the biologic structures responsible for the US effect vary greatly among species. These issues must be carefully explored. Of necessity, there is another limitation to the present study. We examined a rabbit corneal epithelial cell line in an the vitro study, but the gene-transferred cells were mainly keratocytes in the in vivo study. In our preliminary study, rabbit keratocytes were cultured; however, the morphology of these cells soon changed and differentiated into unidentifiable cells. Therefore, we used the rabbit corneal cell line RC-1.

To summarize, our studies show that using US in conjunction with commercially available MBs can enhance gene delivery to cells without damaging tissues. Although this modality was highly dependent on acoustic conditions and bubble concentration, its simplicity and noninvasiveness may provide a new avenue for microinjecting various substances into a wide range of living tissues.

References

1. Marshall E. Gene therapy's growing pains. *Science.* 1995;269:1050, 1052–1055.
2. Felgner PL, Barenholz Y, Behr JP, et al. Nomenclature for synthetic gene delivery systems. *Hum Gene Ther.* 1997;8:511–512.
3. Marshall E. Gene therapy death prompts review of adenovirus vector. *Science.* 1999;286:2244–2245.
4. Hacein-Bey-Abina S, Le Deist F, Carlier F, et al. Sustained correction of X-linked severe combined immunodeficiency by ex vivo gene therapy. *N Engl J Med.* 2002;346:1185–1193.
5. Grisham J. Inquiry into gene therapy widens. *Nat Biotechnol.* 2000;18:254–255.
6. Wolff JA, Malone RW, Williams P, et al. Direct gene transfer into mouse muscle in vivo. *Science.* 1990;247:1465–1468.
7. Wolff JA, Ludtke JJ, Acsadi G, Williams P, Jani A. Long-term persistence of plasmid DNA and foreign gene expression in mouse muscle. *Hum Mol Genet.* 1992;1:363–369.
8. Felgner PL, Gadek TR, Holm M, et al. Lipofection: a highly efficient, lipid-mediated DNA-transfection procedure. *Proc Natl Acad Sci USA.* 1987;84:7413–7417.
9. Stechschulte SU, Joussen AM, von Recum HA, et al. Rapid ocular angiogenic control via naked DNA delivery to cornea. *Invest Ophthalmol Vis Sci.* 2001;42:1975–1979.
10. Nishi T, Yoshizato K, Yamashiro S, et al. High-efficiency in vivo gene transfer using intraarterial plasmid DNA injection following in vivo electroporation. *Cancer Res.* 1996;56:1050–1055.
11. Drabick JJ, Glasspool-Malone J, King A, Malone RW. Cutaneous transfection and immune responses to intradermal nucleic acid vaccination are significantly enhanced by in vivo electropermeabilization. *Mol Ther.* 2001;3:249–255.
12. Newman CM, Lawrie A, Brisken AF, Cumberland DC. Ultrasound gene therapy: on the road from concept to reality. *Echocardiography.* 2001;18:339–347.

13. Kim HJ, Greenleaf JF, Kinnick RR, Bronk JT, Bolander ME. Ultrasound-mediated transfection of mammalian cells. *Hum Gene Ther.* 1996;7:1339–1346.
14. Bao S, Thrall BD, Miller DL. Transfection of a reporter plasmid into cultured cells by sonoporation in vitro. *Ultrasound Med Biol.* 1997;23:953–959.
15. Wyber JA, Andrews J, D'Emanuele A. The use of sonication for the efficient delivery of plasmid DNA into cells. *Pharm Res.* 1997;14:750–756.
16. Miller DL, Williams AR, Morris JE, Chrisler WB. Sonoporation of erythrocytes by lithotripter shockwaves in vitro. *Ultrasonics.* 1998;36:947–952.
17. Lawrie A, Brisken AF, Francis SE, et al. Ultrasound enhances reporter gene expression after transfection of vascular cells in vitro. *Circulation.* 1999;99:2617–2620.
18. Manome Y, Nakamura M, Ohno T, Furuhata H. Ultrasound facilitates transduction of naked plasmid DNA into colon carcinoma cells in vitro and in vivo. *Hum Gene Ther.* 2000;11:1521–1528.
19. McDonnell PJ. Excimer laser corneal surgery: new strategies and old enemies. *Invest Ophthalmol Vis Sci.* 1995;36:4–8.
20. Seitz B, Baktanian E, Gordon EM, Anderson WF, LaBree L, McDonnell PJ. Retroviral vector-mediated gene transfer into keratocytes: in vitro effects of polybrene and protamine sulfate. *Graefes Arch Clin Exp Ophthalmol.* 1998;236:602–612.
21. Bennett J, Maguire AM. Gene therapy for ocular disease. *Mol Ther.* 2000;1:501–505.
22. Wang X, Liang HD, Dong B, Lu QL, Blomley MJ. Gene transfer with microbubble ultrasound and plasmid DNA into skeletal muscle of mice: comparison between commercially available microbubble contrast agents. *Radiology.* 2005;237:224–229.
23. Greenleaf WJ, Bolander ME, Sarkar G, Goldring MB, Greenleaf JF. Artificial cavitation nuclei significantly enhance acoustically induced cell transfection. *Ultrasound Med Biol.* 1998;24:587–595.
24. Lu QL, Bou-Gharios G, Partridge TA. Non-viral gene delivery in skeletal muscle: a protein factory. *Gene Ther.* 2003;10:131–142.
25. Blomley M. Which US microbubble contrast agent is best for gene therapy? *Radiology.* 2003;229:297–298.
26. Lawrie A, Brisken AF, Francis SE, Cumberland DC, Crossman DC, Newman CM. Microbubble-enhanced ultrasound for vascular gene delivery. *Gene Ther.* 2000;7:2023–2027.
27. Shohet RV, Chen S, Zhou YT, et al. Echocardiographic destruction of albumin microbubbles directs gene delivery to the myocardium. *Circulation.* 2000;101:2554–2556.
28. Unger EC, Hersh E, Vannan M, McCreery T. Gene delivery using ultrasound contrast agents. *Echocardiography.* 2001;18:355–361.
29. Taniyama Y, Tachibana K, Hiraoka K, et al. Local delivery of plasmid DNA into rat carotid artery using ultrasound. *Circulation.* 2002;105:1233–1239.
30. Taniyama Y, Tachibana K, Hiraoka K, et al. Development of safe and efficient novel nonviral gene transfer using ultrasound: enhancement of transfection efficiency of naked plasmid DNA in skeletal muscle. *Gene Ther.* 2002;9:372–380.
31. Lu QL, Liang HD, Partridge T, Blomley MJ. Microbubble ultrasound improves the efficiency of gene transduction in skeletal muscle in vivo with reduced tissue damage. *Gene Ther.* 2003;10:396–405.
32. Nakashima M, Tachibana K, Iohara K, Ito M, Ishikawa M, Akamine A. Induction of reparative dentin formation by ultrasound-mediated gene delivery of growth/differentiation factor 11. *Hum Gene Ther.* 2003;14:591–597.
33. Vincent MC, Trapnell BC, Baughman RP, Wert SE, Whitsett JA, Iwamoto HS. Adenovirus-mediated gene transfer to the respiratory tract of fetal sheep in utero. *Hum Gene Ther.* 1995;6:1019–1028.
34. Porada CD, Tran N, Eglitis M, et al. In utero gene therapy: transfer and long-term expression of the bacterial neo(r) gene in sheep after direct injection of retroviral vectors into preimmune fetuses. *Hum Gene Ther.* 1998;9:1571–1585.
35. Oshima Y, Sakamoto T, Hisatomi T, et al. Targeted gene transfer to corneal stroma in vivo by electric pulses. *Exp Eye Res.* 2002;74:191–198.
36. Oshima Y, Sakamoto T, Hisatomi T, Tsutsumi C, Ueno H, Ishibashi T. Gene transfer of soluble TGF-beta type II receptor inhibits experimental proliferative vitreoretinopathy. *Gene Ther.* 2002;9:1214–1220.
37. Sakamoto T, Oshima Y, Nakagawa K, Ishibashi T, Inomata H, Sueishi K. Target gene transfer of tissue plasminogen activator to cornea by electric pulse inhibits intracameral fibrin formation and corneal cloudiness. *Hum Gene Ther.* 1999;10:2551–2557.
38. Tachibana K, Tachibana S. Transdermal delivery of insulin by ultrasonic vibration. *J Pharm Pharmacol.* 1991;43:270–271.
39. Tachibana K, Uchida T, Ogawa K, Yamashita N, Tamura K. Induction of cell-membrane porosity by ultrasound (Letter). *Lancet.* 1999;353:1409.
40. Tachibana K, Tachibana S. The use of ultrasound for drug delivery. *Echocardiography.* 2001;18:323–328.

J Med Ultrasonics (2006) 33:■■–■■
DOI 10.1007/s10396-005-0066-7

ORIGINAL ARTICLE

Go KAGIYA · Yoshiaki TABUCHI · Loreto B. FERIL Jr.
Ryohei OGAWA · Qing-Li ZHAO · Nobuki KUDO
Wakako HIRAOKA · Katsuro TACHIBANA
Shin-ichiro UMEMURA · Takashi KONDO

Confirmation of enhanced expression of heme oxygenase-1 gene induced by ultrasound and its mechanism: analysis by cDNA microarray system, real-time quantitative PCR, and Western blotting

Received: June 3, 2005 / Accepted: July 26, 2005

Abstract
Purpose. The present study was undertaken to reconfirm heme oxygenase-1 (HO-1) induction by ultrasound, and elucidate the mechanism by which this occurs.
Methods. After exposure of human lymphoma U937 cells to 1 MHz continuous ultrasound (US), gene profiling by using cDNA microarray analysis, cell viability by using the trypan blue dye exclusion test, mRNA expression by using real-time quantitative polymerase chain reaction, and protein expression by using Western blotting were examined. As an indicator of cavitation, hydroxyl radical formation was studied by using electron paramagnetic resonance-spin trapping.
Results. The cDNA microarray analysis reconfirmed HO-1 induction in human lymphoma U937 cells after exposure to US, and further identified one upregulated and two downregulated genes. When U937 cells were exposed to US for 1 min, HO-1 induction, as examined by real-time quantitative polymerase chain reaction and Western blotting, was observed at intensities higher than the cavitational threshold. When a potent antioxidant, *N*-acetyl-L-cysteine, was added to the culture medium before or after sonication, the induction was attenuated, indicating that reactive oxygen species are involved in HO-1 induction. A decrease in mitochondrial membrane potential and generation of superoxide anion radicals were also observed in the cells exposed to US.
Conclusion. We used a cDNA microarray system to confirm upregulation of the *HO-1* gene and to discover new genes that respond to ultrasonic cavitation. Increased intracellular oxidative stress secondary to the sonomechanical effects arising from ultrasonic cavitation is suggested to be the mechanism of enhancement of *HO-1* expression.

Keywords cDNA microarray · gene profiling · heme oxygenase-1 · ultrasonic cavitation

G. Kagiya · L. B. Feril Jr. · R. Ogawa · Q.-L. Zhao · T. Kondo (✉)
Department of Radiological Sciences, Faculty of Medicine, Toyama Medical and Pharmaceutical University, 2630 Sugitani, Toyama 930-0194, Japan
Tel. +81-76-434-7265; Fax +81-76-434-5190
e-mail: kondot@ms.toyama-mpu.ac.jp

G. Kagiya
The Wakasa-wan Energy Research Center, Tsuruga, Japan

Y. Tabuchi
Division of Molecular Genetics Research, Life Science Research Center, Toyama Medical and Pharmaceutical University, Toyama, Japan

N. Kudo
Laboratory of Biomedical Instrumentation and Measurement, Graduate School of Information Science and Technology, Hokkaido University, Sapporo, Japan

W. Hiraoka
Department of Physics, School of Science and Technology, Meiji University, Kawasaki, Japan

K. Tachibana
Department of Anatomy, Fukuoka University School of Medicine, Fukuoka, Japan

S. Umemura
School of Health Sciences, Faculty of Medicine, Kyoto University, Kyoto, 606-8507 Japan

G. K. and Y. T. contributed equally to this work.

Introduction

Ultrasound has been used for diagnosis and therapy in many medical fields. The biophysical modes of ultrasonic action are classified as thermal, cavitational and nonthermal noncavitational effects.[1,2] Cavitation is known to lead to both mechanical shear stress and free radical formation arising from the collapse of oscillating bubbles. Hydroxyl radicals and hydrogen atoms form as a result of the thermal dissociation of water induced by very high temperatures (several thousand degrees Kelvin) and pressures in several micron sizes within a few microseconds arising from cavitation bubble collapse.[3–5] In general, it has been inferred that these two effects (chemical effects due to free radicals and mechanical effects due to shear stress) of cavitation act simultaneously on biological materials. It is well known that

ultrasonic cavitation induces disruption of the cellular membrane, causing irreversible cellular damage resulting in instant cell lysis and necrosis. Recent reports indicate that cavitation also can induce apoptosis, that is, gene-regulated cell death, which has uniquely defined morphological and molecular characteristics.[6–11]

Novel transcript profiling technologies such as cDNA microarray analysis allow the simultaneous measurement of changes in expression of many hundreds or many thousands of genes.[12,13] We have already applied cDNA microarray profiling to the analysis of gene expression in biological experiments.[14–16] This technology is also useful for the identification of specifically expressed genes induced by physical and chemical stress.

In our previous study, gene expression of intact human lymphoma U937 cells 6h after ultrasonic exposure was examined by cDNA microarray profiling to identify genes responsive to ultrasonic cavitation. Of the 9182 human genes examined, five genes, including heme oxygenase-1 (*HO-1*), were upregulated and two genes were downregulated in cells exposed to ultrasound in the presence of Ar gas, where cell lysis and apoptosis were observed. Among these genes, *HO-1* was the most upregulated (up to 6.6-fold) as confirmed by semiquantitative reverse transcription–polymerase chain reaction (RT-PCR).[17]

The present study was performed to reconfirm the upregulation of *HO-1* induced by ultrasound and to clarify the mechanism of *HO-1* induction in cultured human lymphoma cells. The biological significance of the *HO-1* gene expression induced by ultrasound is also discussed.

Materials and methods

Cells and cell culture

The human myelomonocytic lymphoma cell line (U937) used in the present study was obtained from the Human Sciences Resources Bank (Human Sciences Foundation, Tokyo, Japan). The cells were maintained in RPMI-1640 culture medium supplemented with 10% heat-inactivated fetal bovine serum (FBS; JRH Biosciences, Lenexa, KS, USA) at 37°C in humidified air with 5% CO_2. Cell viability before treatment was always more than 95%.

The prostatic cancer cell lines DU145 and LNCap, and leukemia cell lines Jurkat and K562 were maintained in RPMI-1640 culture medium supplemented with heat-inactivated 10% FBS at 37°C in humidified air with 5% CO_2. A mouse leukemic monocyte cell line (RAW 264) was also used in the present study and was maintained in Dulbecco's modified Eagle's culture medium supplemented with 10% heat-inactivated FBS and with 1% nonessential amino acids (Invitrogen Japan, Tokyo, Japan) at 37°C in humidified air with 5% CO_2.

Reagents

A spin trap reagent, 5,5-dimethyl-1-pyrroline 1-oxide (DMPO), was purchased from Labotec (Tokyo, Japan). *N*-acetyl-L-cysteine (NAC) and catalase were purchased from Sigma-Aldrich (Tokyo, Japan). Fluorescent dyes, 3,3′-dihexyloxacarbocyamine iodide ($DiOC_6(3)$) and dihydroethidium (HE), were obtained from Molecular Probes (Eugene, OR, USA), and other reagents were purchased from Wako Pure Chemical Industries (Osaka, Japan).

Ultrasonic apparatus and condition of sonication

Two types of ultrasonic exposure systems were used: rotating tubes with relatively high intensities or culture dishes with relatively low intensities.

The rotating tube ultrasonic apparatus consisted of an acrylic tank and an unfocused ceramic transducer (3 cm diameter) driven by a 1.0-MHz ultrasonic generator.[18] Sonication was carried out using a disposable sterile culture tube (no. 25760; Corning, Corning, NY, USA), for which it was reported that the attenuation is approximately 35% with only the front half of the tube. Although the culture tubes cause considerably more perturbation of the sound field because of the standing waves, the arrangement of the rotation tube system was effective for producing cavitation and was useful for homogeneous exposure. When the sample solution was transferred into the tube, the 3.5 ml of sample formed a column 3 cm high. The tube was positioned directly in front of the transducer face with the tube axis 20 cm from the transducer. During sonication, the tube was rotated at 30 rpm by a synchronous motor to improve mixing and to provide more uniform exposure. Ultrasonic intensities were measured by using a stainless-steel ball radiometer.[18] Cells were sonicated for 1 min at an intensity of 3.6 W/cm^2 [spatial-average and temporal-average intensity (I_{SATA})].

The culture dish ultrasonic exposure system comprised an acrylic water tank, an ultrasonic generator (KUS-2S; Ito Ultrasonic, Tokyo, Japan) and an unfocused ceramic transducer (2.7 cm diameter). Cell suspension (2 ml) in a 35-mm culture dish was fixed by a holder at 20 mm above the transducer face and sonicated with 1.0-MHz ultrasound upward. For measurement of ultrasonic intensity, an ultrasound power meter (UPM-DT-10E; Ohmic Instruments, Easton, MD, USA) was used, and I_{SATA} was obtained from the effective power (W) divided by the surface area (5.7 cm^2) of the transducer. Cells were sonicated at intensities of 0.1, 0.3, 0.8, 1.1, 1.4, and 1.6 W/cm^2 (I_{SATA}), mostly at an intensity of 1.1 W/cm^2. Surrounding water in the acrylic tank was kept at 37.0°C.

Treatment with H_2O_2 and $CdCl_2$, and X-irradiation

Cells were treated with H_2O_2 at a concentration of 600 μM, and with $CdCl_2$ at a concentration of 5 μM for 6h, after which they were harvested for Western blotting.

X-irradiation was carried out at room temperature by using an X-ray apparatus (MBR-1520R-3; Hitachi Medico Technology, Kashiwa, Japan) operating at 150 kVp and 20 mA at a dose rate of 5 Gy/min as determined by a Fricke dosimeter. Cells in a 6-cm culture dish were exposed to X-rays and incubated for 6 h in a CO_2 incubator, after which they were harvested for Western blotting.

Measurement of cell survival

After sonication, cells could be divided into three groups: (1) cells that were completely lysed; (2) cells that could be stained by trypan blue; and (3) cells that were intact and not stained by trypan blue. Immediately after sonication, a 0.4% trypan blue solution was added to aliquots of cell suspensions to a final concentration of 0.04% to estimate the number of cells in the third group, the cells of which are referred to as "intact and viable" cells. The survival rate (%) immediately after sonication is given as the fraction of "intact and viable" cells.

Electron paramagnetic resonance spin trapping for the detection of free radical formation

Because free radical formation in water by ultrasound is an indicator of the occurrence of inertial cavitation during sonication,[5] we used electron paramagnetic resonance (EPR) spin trapping, using DMPO as the spin trap. As a nitrone spin trap, DMPO reacts with hydroxyl radicals and hydrogen atoms, producing DMPO-OH and DMPO-H adducts, respectively. However, DMPO-H is relatively short lived (its half life is approximately 60 s at pH 7.0). Therefore, DMPO can be used as a useful spin trap for detecting hydroxyl radicals only. An aqueous solution containing DMPO at a concentration of 10 mM was saturated with argon gas by bubbling at a flow rate of 100 ml/min for more than 15 min and sonicated for 1 min. Immediately after sonication, the sonicated solution was transferred to a quartz-flat cell, and the EPR spectra of the sample was recorded with an EPR apparatus (RFR-30; Radical Research, Tokyo, Japan) using 9.452-GHz field modulation with a 0.1-mT amplitude with a microwave power of 4 mW at room temperature. The yields of spin adduct were determined by using a stable nitroxide radical, TEMPOL (4-hydroxyl-2,2,6,6-tetramethyl-1-piperidinyloxy), as a standard. A calibration curve was determined by plotting the product of the peak-to-peak derivative amplitude and the square of the width at maximum slope of the signal versus the different concentrations of the standard nitroxide radical. In Fig. 1, one unit of the Y-axis (DMPO-OH EPR signal) is calculated to be approximately 19.0 μM of TEMPOL (relative value based on the standard).

Separation of total RNA and mRNA

Total RNA was extracted from the U937 cells using an RNeasy Total RNA Extraction Kit (Qiagen, Tokyo, Japan).

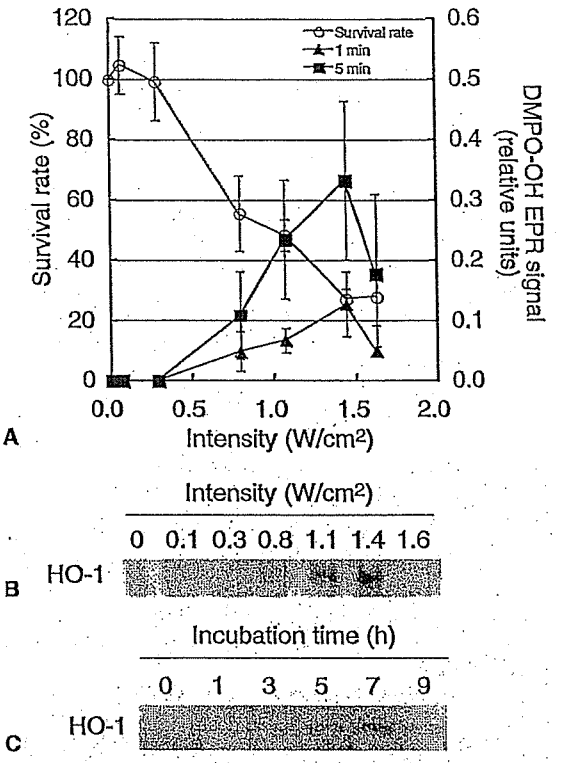

Fig. 1. **a** Effects of ultrasonic intensity on cell survival (*open circle*) and hydroxyl radical formation (*filled symbols*) induced by ultrasound (data are mean ± SD). **b** Western blot analysis of the effects of ultrasonic intensity on HO-1 expression induced by ultrasound. **c** Time course of HO-1 expression after sonication for 60 s with 1.0-MHz continuous wave at 1.1 W/cm²

RNA samples were treated with RNase-free DNase (Qiagen) for 30 min at room temperature. mRNAs were extracted from the DNase-treated samples using a GenElute-mRNA Miniprep Kit (Sigma-Aldrich, St. Louis, MO, USA).

cDNA microarray analysis

cDNA microarray analysis was performed by using human glass microarrays (IntelliGene II Human CHIP 1; Takara Bio, Shiga, Japan), which were spotted with 3,893 cDNA fragments of human genes. cDNA probes were prepared by RT reaction with Cy3-dUTP (Amersham Pharmacia Biotech, Tokyo, Japan) or Cy5-dUTP (Amersham Pharmacia Biotech) from mRNAs from the U937 cells treated with or without ultrasound (6 h after the treatment), respectively, by using an RNA Fluorescence Labeling Core Kit (Takara Bio). In some experiments, a control sample was labeled with Cy5, and in others, it was labeled with Cy3, with essen-

tially identical results. After treatment with RNase H, cDNA probes were purified by gel filtration. Hybridization and washing of the microarray were carried out according to the manufacturer's instructions. In brief, cDNA probe solutions containing both Cy3- and Cy5-labeled cDNA probes were applied to the microarrays, and the microarrays were covered with a spaced glass cover slip (Takara Bio) and placed in a humidified chamber at 65°C for 16 h. Then, the microarrays were sequentially washed in 2× SSC (150 mM NaCl and 15 mM sodium citrate) containing 0.2% sodium dodecylsulfate (SDS) for 5 min twice at 55°C, in 2× SSC containing 0.2% SDS for 5 min once at 65°C and in 0.05× SSC for 1 min once at room temperature. The microarrays were scanned in both Cy3 and Cy5 channels with a ScanArray Lite (Packard BioChip Technologies, Billerica, MA, USA). QuantArray software (Packard BioChip Technologies) was used for image analysis. Genes were considered to be positively expressed if the signal/background ratio was >3.0. The average of glyceraldehyde 3-phosphate dehydrogenase (G3PDH) Cy3 and Cy5 signals (12 spots each) gave a ratio that was used to balance or normalize the signals.[14–17]

Addition of free radical scavengers

For free radical scavenging, 7.0×10^6 cells were suspended in culture medium containing 0.2 mM of NAC and incubated at 37°C for 1 h. Before sonication, cells were centrifuged and gently resuspended in 4 ml of Ar-saturated medium containing the same scavenger and transferred to a 35-mm culture dish to be sonicated. Cells in a dish were sonicated with 1.0-MHz ultrasound at 1.1 W/cm^2 for 60 s and then incubated at 37.0°C for 7 h after addition of FBS at a concentration of 10%.

Western blotting

Sonicated cells were collected by centrifugation and lysed at room temperature for 15 min in Passive Lysis Buffer (Promega, Madison, WI, USA) after being washed in phosphate-buffered saline (PBS) twice. The protein concentration of the centrifuged supernatant was measured by using a Protein Assay Kit (Nippon Bio-Rad Laboratories, Tokyo, Japan). After the protein concentrations were standardized, each of the cell lysates was mixed with the same volume of 2× SDS loading buffer (200 mM dithiothreitol, 4% SDS, 0.2% bromophenol blue, 20% glycerol, and 100 mM Tris-HCl, pH 6.8) and boiled at 95°C for 10 min. The samples were electrophoresed on 12% polyacrylamide gel and then transferred onto an immobilon PVDF membrane (Nihon Millipore, Tokyo, Japan). After the membrane was blocked in 5% skim milk in PBS, it was treated with an anti-HO-1 polyclonal antibody (Santa Cruz Biotechnology, Santa Cruz, CA, USA) and a secondary antibody conjugated with alkaline phosphatase (Chemicon International, Temecula, CA, USA). The HO-1 protein band was visualized with CDP-Star (Tropix, Bedford, MA, USA) and recorded on a LAS-1000 chemi-luminescence detector (Fuji Photo Film, Tokyo, Japan).

Real-time PCR analysis

Using an RNeasy Total RNA Extraction Kit (Qiagen), whole cell RNA was extracted from 1.4×10^6 cells, following the manufacturer's instructions. cDNA was synthesized by RT reaction at 37°C for 1 h with an Omniscript Reverse Transcription Kit (Qiagen). For the real-time quantitative PCR reaction, HO-1-F (5′-GAGGGAAGCCCCCACTCA-3′) and HO-1-R (5′-AACTGTCGCCACCAGAAAGCT-3′) were used as primers for HO-1 mRNA, and G3PDH-F (5′-AAGGACTCATGACCACAGTCCAT-3′) and G3PDH-R (5′-CCATCACGCCACAGTTTCC-3′) were used as primers for the inner control, G3PDH. As TaqMan probes, we used HO-1-T (5′-CCGCTCCCAGGCTCCGC TTC-3′) and G3PDH-T (5′-CCATCACTGCCACCCA-GAAGACTGTG-3′) for HO-1 and G3PDH, respectively. The probes were labeled with FAM for the 5′ end and TAMRA for the 3′ end. The reaction mixture, which comprised 1 μg of cDNA, 900 nM of each primer, 200 nM of each TaqMan probe, qPCR Mastermix (Nippon Gene Co., Toyama, Japan), and 5 mM of $MgCl_2$, was used in an ABI Prism 7700 sequence detection system (Applied Biosystems, Foster, CA) for reactions of 40 cycles at 95.0°C for 15 s and at 60.0°C for 60 s preceded by reactions at 50.0°C for 2 min and 95.0°C for 10 min. The ratio of HO-1 inductions was calculated by the following formula: $Y = X_U/X_0$, where X_U is the signal ratio of HO-1 to G3PDH in a sample with sonication and X_0 is the signal ratio of HO-1 to G3PDH in a sample without sonication.

Detection of mitochondrial transmembrane potential and intracellular superoxide formation

We used $DiOC_6(3)$ and HE for detecting the mitochondrial transmembrane potential and intracellular superoxide formation, respectively. After exposure to ultrasound, the cells were incubated for 6 h and collected by centrifugation at 1000× *g* for 3 min. The cells (approximately 1×10^6 cells) were resuspended in PBS containing 1% FBS, and 40 nM $DiOC_6(3)$ or 2 μM HE. They were then incubated at 37°C for 15 min and washed twice in PBS before flow cytometric analysis (FACSCalibur, Nippon Becton Dickinson, Tokyo, Japan).

Statistical analysis

All values are expressed as mean ± standard deviation (SD). Differences were assessed by using Student's unpaired *t* test. Statistical significance was established at a value of $P < 0.01$.

22

Table 1. Up- and downregulated genes after sonication in U937 cells

Gene	Fold change			GenBank accession no.
	Exp. 1	Exp. 2	Average	
Upregulated				
PCTAIRE protein kinase 1 Transcript variant 2 (PCTK1-V2)	2.5	2.1	2.3	NM_033018
Heme oxygenase-1 (HO-1)	3.4	2.4	2.9	NM_002133
Downregulated				
Leukemia inhibitory factor receptor (LIFR)	0.17	0.23	0.20	NM_002310
Chemokine ligand 10 (CXCL10)	0.50	0.43	0.47	NM_001565

Microarray analysis was performed (details of experimental conditions are described in the materials and methods section)
Exp., experiment

Results

cDNA microarray analysis

In order to identify genes that are differentially expressed in U937 cells treated with ultrasound for 1 min at an intensity of 3.6 W/cm², we carried out cDNA microarray analysis of the cells 6 h after ultrasound treatment. Hydroxyl radical formation, the fraction of intact cells, and apoptosis under these experimental conditions have been described in previous reports.[7,17] Genes were considered to be up- or downregulated if the average fold change was 2.0 or greater in duplicate experiments. Of the 3893 genes examined, changes in mRNA levels were detected in four genes: two genes, PCTAIRE protein kinase 1 transcript variant 2 (*PCTK1-V2*) and *HO-1*, were upregulated, whereas two genes, leukemia inhibitory factor receptor (*LIFR*) and chemokine ligand 10 (*CXCL10*), were downregulated by ultrasound treatment. The average fold change of *PCTK1-V2, HO-1, LIFR* and *CXCL10* was 2.3, 2.8, 0.20, and 0.47, respectively (Table 1). Thus, upregulation of *HO-1* was confirmed, and three genes responding to ultrasonic cavitation were identified.

9

Cell survival and free radical formation

When the U937 cells were sonicated for 1 min with graded intensity, the survival rate decreased with increasing intensity except at intensities less than 0.3 W/cm². Furthermore, the relationship between ultrasonic intensity and hydroxyl radical formation, which is an endpoint of inertial cavitation, was studied with EPR spin trapping using DMPO as a spin trap. In a similar manner, the EPR signal of DMPO-OH adducts was not detected at up to 0.3 W/cm², and it increased with increasing intensity up to 1.4 W/cm² (Fig. 1a). At an intensity of 1.6 W/cm², formation of DMPO-OH adduct decreased. The reason or reasons for the decrease are unknown. However, it could be attributed to a rapid degassing effect at high intensity or premature collapse of cavitation at intensities much greater than the threshold of cavitation, meaning that the bubbles cannot gain enough energy from the momentum of oscillation.

Dose response of HO-1 induction

10

When the U937 cells were sonicated for 1 min at graded intensities, HO-1 expression was examined by Western blotting after 7 h. The level of expression increased with increasing intensity up to 1.4 W/cm² (Fig. 1b). Furthermore, the effects of incubation time on HO-1 expression were examined in cells exposed to ultrasound at 1.1 W/cm². HO-1 expression increased with increasing incubation time up to 7 h (Fig. 1c).

Effects of NAC

To verify the involvement of reactive oxygen species (ROS), we sonicated cells with or without NAC, a broad-range scavenger of ROS, and measured HO-1 expression by using real-time quantitative PCR. As shown in Fig. 2, the fold induction of HO-1 expression in the sonicated samples without NAC was 25.7 ± 11.2 (mean ± SD; n = 21), whereas that of sonicated samples in the presence of 200 μM NAC was 2.2 ± 0.7 (mean ± SD; n = 4). This showed that addition of NAC suppressed the induction of HO-1 expression, affirming the role of ROS. In addition, even when NAC was added immediately after sonication, HO-1 induction was still suppressed in a manner comparable to that observed in cells treated with NAC before sonication (mean ± SD 2.2 ± 0.6; n = 3), suggesting the involvement of ROS generated intracellularly after sonication or the formation of ROS with long half-lives such as hydrogen peroxide.

11

Change in mitochondrial transmembrane potential and superoxide formation

To examine the source of ROS involved in HO-1 induction, change in mitochondrial transmembrane potential and

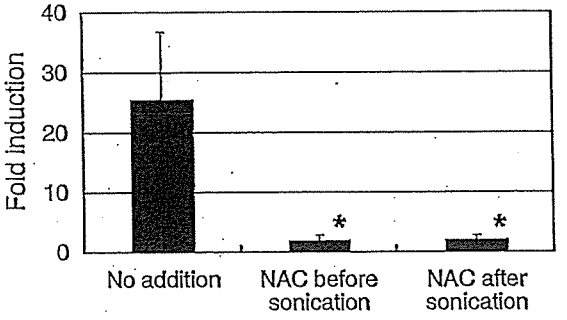

Fig. 2. Effects of an antioxidant, *N*-acetyl-l-cysteine (NAC), on HO-1 expression induced by ultrasound. U937 cells were pre-incubated in medium containing 0.2 mM of NAC for 1 h and then sonicated for 60 s with 1.0-MHz continuous wave at 1.1 W/cm², or were treated with NAC immediately after sonication and incubated for 7 h. HO-1 expression was examined by real-time quantitative PCR. The ratio of HO-1 induction to that in a sample without sonication was determined and expressed as fold induction. The error *bars* in the figure are the standard deviations ($n = 3$). *Asterisks* indicate a statistically significant difference relative to ■■ ($P < 0.01$)

19

superoxide formation was estimated by using the fluorescent probes $DiOC_6(3)$ and HE, respectively. For measurement of mitochondrial transmembrane potential, the fraction (%) of cells with low mitochondrial transmembrane potential in control samples was 9.3 ± 15.1 (mean ± SD, $n = 3$). However, that of sonicated samples was 46.1 ± 5.6 (mean ± SD, $n = 3$) 6 h after sonication (Fig. 3). Similarly, the fraction (%) of cells with superoxide formation in control samples was 7.2 ± 2.6 (mean ± SD, $n = 3$), whereas that in sonicated samples was 66.3 ± 1.2 (mean ± SD, $n = 3$) 6 h after sonication (Fig. 3). These results clearly indicate mitochondrial dysfunction and superoxide formation in the sonicated cells.

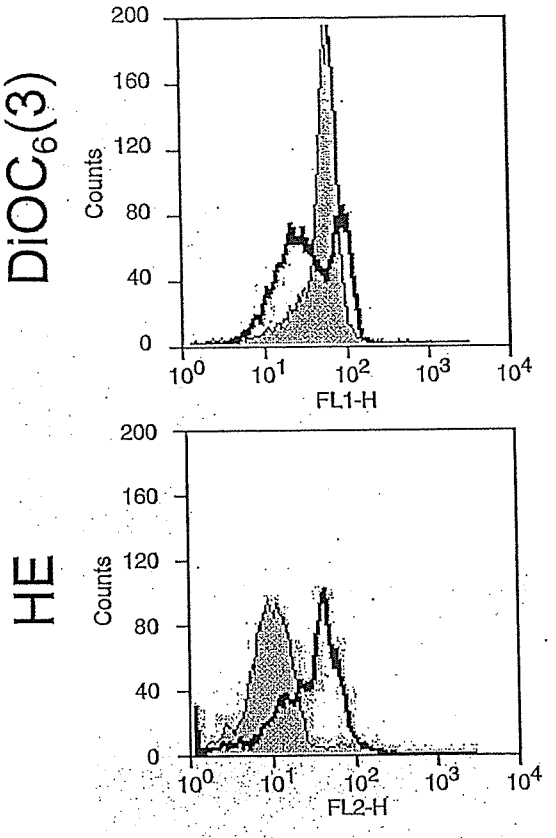

Fig. 3. Change in mitochondrial transmembrane potential and generation of intracellular superoxide after sonication. U937 cells were sonicated for 60 s with 1.0-MHz continuous wave at 1.1 W/cm². The cells were harvested 6 h after sonication and stained with 40-nM $DiOC_6(3)$ or 2-mM HE for flow cytometric analysis. The *gray area* shows the distribution of cells without sonication and the *solid line* shows that of the sonicated cells

HO-1 induction in a variety of cell lines

To obtain comprehensive data on HO-1 induction by ultrasound, human prostatic cancer cell lines (DU145 and LNCap), human leukemia cell lines (Jurkat and K562) and a mouse leukemic monocyte cell line (RAW 264) were also used. These five kinds of cells were sonicated for 1 min with an intensity of 1.1 W/cm², and HO-1 protein expression was examined after 7 h. HO-1 was clearly induced in DU145 and Jurkat cells, but not in the others (Fig. 4).

HO-1 induction by H_2O_2, Cd, and X-irradiation

12 13

The U937 cells were treated with H_2O_2 at a concentration of 600 μM, and with $CdCl_2$ at a concentration of 5 μM, for 6 h, after which they were harvested for Western blotting. Both agents clearly induced the protein expression of HO-1 in U937 cells (Fig. 5a). X-irradiation also induced expression depending on the radiation dose. These results indicate that oxidative stress, H_2O_2, Cd ions, and X-irradiation induce HO-1 in U937 cells (Fig. 5b).

G

Discussion

Previously, using cDNA microarray and semi-quantitative RT-PCR techniques, we analyzed changes in the gene expression of U937 cells in a medium saturated with Ar after sonication with a 1.0-MHz continuous wave. We found that the *HO-1* gene was related to the cavitation-mediated mechanism and was upregulated 6.6-fold, which was the highest upregulation among the genes investigated.[17] In the present study, first we used a cDNA microarray system to confirm and discover new genes that respond to ultrasonic cavitation. Second, we used real-time quantitative PCR and Western blotting techniques to explore the mechanism of *HO-1* upregulation. The results reconfirmed *HO-1* upregu-